# Layer Recurrent Neural Network Solution for an Electromagnetic Interference Problem

Dan D. Micu[1], Levente Czumbil[1], Georgios Christoforidis[2], and Andrei Ceclan[1]

[1]Electrical Engineering Department, Technical University of Cluj Napoca, Romania
[2]Electrical Engineering Department, Technological Institute of West Macedonia, Greece

**The paper presents an original contribution related to the implementation of a neural network artificial intelligence (AI) technique through Matlab environment, on the study of induced AC voltage in the underground metallic pipeline, due to nearby high voltage grids. The advantage yields in a simplified computation model compared to FEM, and implicitly a lower computational time. In comparison with other neural network solutions identified in the literature, where the induced AC potential is directly evaluated, the authors of this paper propose a new neural network solution to evaluate MVP on the studied domain, using a larger training database for a large panel of different geometries.**

***Index Terms*—Electromagnetic compatibility, electromagnetic fields, finite element method, neural networks, pipelines, transmission lines.**

## I. Introduction

CURRENTLY, to reduce construction costs of underground metallic pipelines (designed to transport liquid or gaseous substances like oil, water, gas, etc.) they are placed in the same distribution corridor as power system transmission lines. Due to electromagnetic interference between high voltage (HV) power lines (PL) and these metallic pipelines (MP), induced AC potentials will appear. This AC voltage may be dangerous on both the operating personal and on the structural integrity of MP, last due to corrosive effects of the induced current [1]

Usually the electromagnetic interference problems are studied with the finite element method (FEM). In order for this method to be applied on electromagnetic interference problems, it is known that it requires expensive computation time, because a new mesh is required for each construction geometry considered. Therefore, it may be of interest a scaling method of the results from one configuration case to another, so as to provide a lower computational time. [2], [3] Thus, an artificial intelligence based method is presented with emphasize on the input variables and on the architecture of the neural network.

## II. Electromagnetic Interference Problem

We proposed the evaluation of the magnetic vector potential (MVP) on the surface of MP, where the geometry of the electromagnetic interference problem (HVPL and sky wires) is the one presented in [1]. The calculated MVP will be used to determine the induced AC potential in the metallic pipeline.

Fig. 1 shows the cross section of the HVPL-MP common distribution corridor. The problem refers to a buried metallic gas pipeline which shares for 25 [km] the same distribution corridor with a 145 kV/50 [Hz] frequency HVPL. The transmission line consists in HAWK ACSR conductors and two 4 mm radius sky wires.

End effects are neglected for the inductive interference calculations, therefore leading to a two dimensional problem.

Manuscript received May 29, 2010; accepted October 26, 2010. Date of current version April 22, 2011. Corresponding author: D. D. Micu (e-mail: Dan.Micu@et.utcluj.ro).

Color versions of one or more of the figures in this paper are available online at http://ieeexplore.ieee.org.

Digital Object Identifier 10.1109/TMAG.2010.2091494

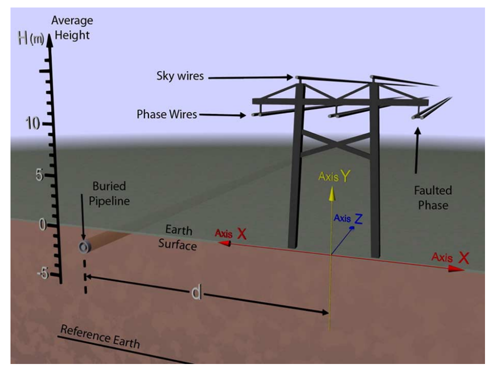


Fig. 1. Cross section of the system under investigation.

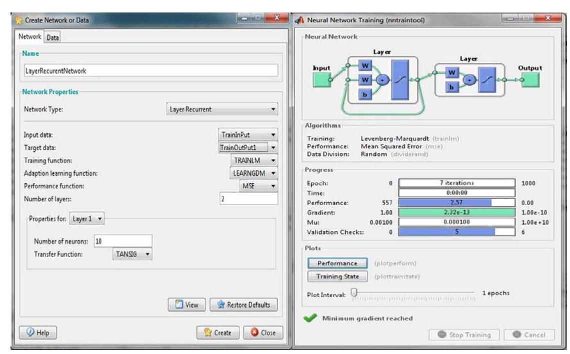

Fig. 2. Implementation and training of the proposed NN.

The HVPL-MP system is represented by a two dimensional problem, which depends on the separation distance $d$, soil resistivity $\rho$ and $(x, y)$ coordinates of the point where the MVP has to be determined. The previous assumption leads to a linear two-dimensional electromagnetic diffusion problem, for the $z$-direction components of MVP and the total current density vector.

Thus, taking into account the cross section of the studied problem, the $z$-direction component of the magnetic vector potential $A_z$ and of the total current density $J_z$ are described by the following equation system:

$$\begin{cases} \frac{1}{\mu_0 \mu_r} \cdot \left[ \frac{\partial^2 A_z}{\partial x^2} + \frac{\partial^2 A_z}{\partial y^2} \right] - j\omega\sigma A_z + J_{sz} = 0 \\ -j\omega\sigma A_z + J_{sz} = J_z \\ \iint\limits_{S_i} J_z ds = I_i \end{cases} \tag{1}$$

where $\sigma$ is the conductivity, $\omega$ is the angular frequency, $\mu_0$ is the magnetic permeability of free space, $\mu_r$ is the relative permeability of the environment, $J_{sz}$ is the source current density in the $z$-direction and $I_i$ is the imposed current on conductor $i$ of $S_i$ cross section. MVP values in every node of the mesh, as well as the unknown current density sources are calculated using the matrix equation solution [1].

Assuming a homogeneous *Dirichlet* boundary condition for the MVP, far away from the system that encloses all the flowing currents, a square with 10 [km] side is set as the total solution domain for the problem. A local error estimator, based on the discontinuity of the instantaneous tangential components of the magnetic field, has been chosen as in [4] for an iteratively adaptive mesh generation.

Bundled conductors are treated as a single conductor of arbitrary shape, by assigning the same material proprieties to all conductors in the bundle.

## III. Neural Network Solution

In comparison with the neural network proposed in [2] and [3], the authors of this paper approach a neural network to calculate the MVP on the studied domain, using a larger training database, in order to obtain more accurate results. The induced voltage is not computed directly, but through MVP.

To gain solutions with a higher accuracy in a shorter training time and with fewer training data, we proposed two different layer recurrent NN, one to calculate the magnitude and the other to calculate the phase of MVP. We chose a layer recurrent NN to obtain a better correlation between the input data and the desired output data through the training process, because these neural networks have the propriety that all the neurons expect that the ones from the output layer take as input value their own output.

These two NN have as input values the four basic parameters which describe the presented 2D problem: $d$ the separation distance between HVPL and MP; $\rho$ the resistivity of the earth; $x$, $y$ coordinates of the point where we wish to compute the MVP.

For each of the two neural networks, a two layers architecture was implemented (an output and a hidden layer). For the hidden layer, 20 neurons were used with a hyperbolic tangent transfer function. For the output layer, we used a neuron with linear transfer function. The number of the neurons on the hidden layer and the used transfer function were determined experimentally by implementing and testing different NN architectures. The two proposed NN were implemented using the graphical user interface (GUI) of the *Neural Network* toolbox in MatLab software.

To train the two proposed NN, we used the solutions given in Table I and obtained with FEM in [5] for different problem geometries. The training time was around 20 to 30 seconds in each case, on a T6400 Intel Core2 Duo processor PC, with a 64 bit operating system, and 4 GB RAM memory.

After training the two neural networks, we verified the provided solutions by comparing the results obtained through the neural network method, with the ones provided in [5] by FEM computation. The comparison was done for the training data set and also for a different testing data set in Table II.

The results are presented in graphical form of the absolute deviation between the solutions given by the implemented neural networks and those provided by FEM, in Figs. 3–6.

TABLE I
DATA BASE USED ***to Train*** THE NEURAL NETWORKS

| No | *d* [m] | *x* [m] | *y* [m] | $\rho$ [Ωm] | MVP Amp. $10^{-5}$ [Wb/m] | MVP Phase [°] |
|---|---|---|---|---|---|---|
| 1 | 70 | 70 | -15 | 30 | 36.1 | -22.8 |
| 2 | 100 | 100 | -30 | 30 | 29.9 | -31.23 |
| 3 | 800 | 770 | -30 | 30 | 4.23 | -82.64 |
| 4 | 800 | 785 | 0 | 30 | 4.27 | -78.83 |
| 5 | 1000 | 1030 | -15 | 30 | 2.48 | -90.27 |
| 6 | 2000 | 1970 | -22.5 | 30 | 0.476 | -108.1 |
| 7 | 2000 | 2020.69 | -8.61 | 30 | 0.436 | -108.54 |
| 8 | 400 | 384.81 | -7.82 | 70 | 17.2 | -44.46 |
| 9 | 400 | 424.77 | -6.93 | 70 | 15.8 | -46.72 |
| 10 | 1000 | 970 | -15 | 70 | 5.95 | -73.04 |
| 11 | 1000 | 1007.5 | 0 | 70 | 5.68 | -72.98 |
| 12 | 1000 | 1015 | -30 | 70 | 5.47 | -76.05 |
| 13 | 70 | 40 | -15 | 100 | 53.8 | -19.34 |
| 14 | 70 | 40 | 0 | 100 | 55.9 | -18.53 |
| 15 | 100 | 92.25 | -25.56 | 100 | 41.5 | -23.98 |
| 16 | 800 | 770 | 0 | 100 | 10.4 | -59.87 |
| 17 | 1000 | 1015 | -30 | 100 | 7.16 | -69.22 |
| 18 | 1000 | 1022.5 | 0 | 100 | 7.23 | -67.27 |
| 19 | 300 | 312.38 | -8.1 | 300 | 31.7 | -28.23 |
| 20 | 300 | 324.05 | -23.53 | 300 | 31 | -30 |
| 21 | 2000 | 2007.5 | 0 | 300 | 5.86 | -72.55 |
| 22 | 300 | 281.66 | -27.03 | 500 | 37.5 | -25.93 |
| 23 | 300 | 290.36 | -15.8 | 500 | 37.1 | -26.01 |
| 24 | 300 | 322.5 | 0 | 500 | 35.5 | -26.74 |
| 25 | 1000 | 1030 | -15 | 500 | 17 | -44.6 |
| 26 | 150 | 120 | -15 | 700 | 54.6 | -19.26 |
| 27 | 400 | 384.81 | -7.82 | 700 | 35.2 | -26.89 |
| 28 | 700 | 690.36 | -15.8 | 700 | 25.6 | -34.07 |
| 29 | 700 | 712.38 | -8.1 | 700 | 25.1 | -34.41 |
| 30 | 150 | 150.55 | -16.99 | 900 | 53 | -19.7 |
| 31 | 200 | 194.77 | -6.93 | 900 | 48.8 | -20.9 |
| 32 | 800 | 830 | -30 | 900 | 24.6 | -35.01 |
| 33 | 1500 | 1499.09 | -17.48 | 900 | 15.6 | -46.35 |
| 34 | 70 | 54.81 | -7.82 | 1000 | 70.3 | -15.94 |
| 35 | 150 | 131.66 | -27.03 | 1000 | 55.8 | -18.98 |
| 36 | 500 | 524.05 | -23.53 | 1000 | 32.9 | -28.27 |
| 37 | 2000 | 2030 | -15 | 1000 | 12.2 | -52.73 |

TABLE II
DATA BASE USED ***to Test*** THE NEURAL NETWORKS

| No | *d* [m] | *x* [m] | *y* [m] | $\rho$ [Ωm] | MVP Amp. $10^{-3}$ [Wb/m] | MVP Phase [°] |
|---|---|---|---|---|---|---|
| 1 | 70 | 81.66 | -27.03 | 30 | 32.9 | -25.57 |
| 2 | 800 | 818.25 | -13.5 | 30 | 3.88 | -82.61 |
| 3 | 400 | 392.25 | -25.56 | 70 | 16.7 | -46.05 |
| 4 | 70 | 40 | -30 | 100 | 50.9 | -20.45 |
| 5 | 1000 | 980.55 | -16.99 | 100 | 7.58 | -67.1 |
| 6 | 200 | 215 | -30 | 500 | 41.8 | -23.83 |
| 7 | 700 | 670 | -22.5 | 700 | 26 | -33.74 |
| 8 | 1500 | 1524.77 | -6.93 | 900 | 15.4 | -46.56 |

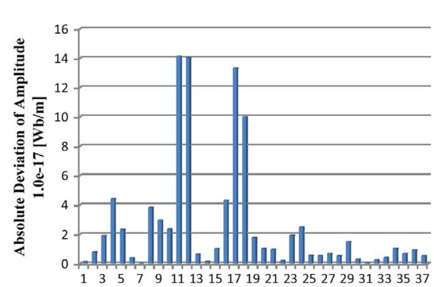


Fig. 3. Absolute deviation of magnitude for the training data.

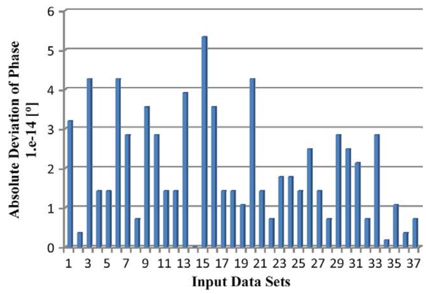


Fig. 4. Absolute deviation of phase for the training data.

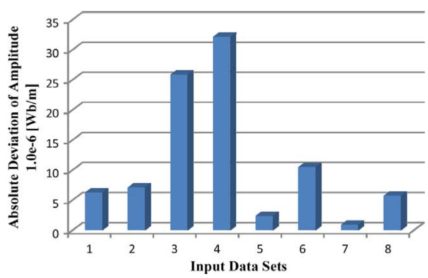


Fig. 5. Absolute deviation of magnitude for the testing data.

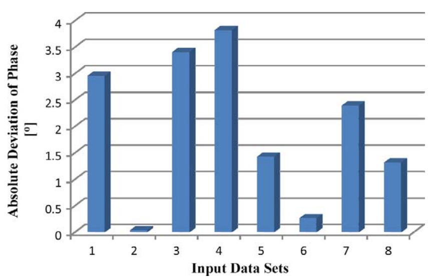


Fig. 6. Absolute deviation of phase for the testing data.

From Figs. 3 and 4, one can observe that for the training data, the yielded NN solution provides accurate numerical values, reflected in the absolute deviation, the difference from the FEM results being insignificant.

For the testing data, the absolute deviation between the NN and FEM results in a higher difference than the previous one, but it is still small enough, so as to be neglected (deviation values under 3.5e-05 [Wb/m] for the magnitude and under 4 degrees for the phase).

## IV. Induced Voltages

To evaluate the induced voltage in the underground metallic pipeline, we used an equivalent electrical circuit model with concentrated elements, with the self and mutual inductances being calculated by classical formulation.

The magnetic vector potential determined with the proposed neural networks on the surface of the metallic structures, which compose the studied problem, is used to evaluate the self and mutual inductances between these metallic components through relations (2) and (3) presented in detail in [1]. If a certain base fault current is imposed on the faulted phase, for example $\overline{I}_{Fb} = 1000$ [A], with the pipeline current $\overline{I}_P$ set equal to zero, the mutual inductance on the pipeline will be:

$$L_{mut} = \frac{\overline{A}_z \cdot l_m}{\overline{I}_{Fb}} \tag{2}$$

TABLE III
Self Inductances for a Case With $\mathrm{d} = 30$ [m] and $\rho = 1000$ [$\Omega$m]

| Component | Self Inductance per unit length $10^{-7}$ [H/m] |
|---|---|
| Phase Conductor 1 (Ph1) | 25.30036-1.48405j |
| Phase Conductor 2 (Ph2) | 25.29659-1.48402j |
| Phase Conductor 3 (Ph3) | 25.34877-1.48400j |
| Sky Wire 1 (Sk1) | 78.93046-1.48048j |
| Sky Wire 2 (Sk2) | 78.87058-1.48045j |
| Pipeline (MP) | 22.15535-1.50061j |

TABLE IV
Self Inductances for a Case With $\mathrm{d} = 500$ [m] and $\rho = 100$ [$\Omega$m]

| Component | Self Inductance per unit length $10^{-7}$ [H/m] |
|---|---|
| Phase Conductor 1 (Ph1) | 23.05461-1.52179j |
| Phase Conductor 2 (Ph2) | 23.05971-1.52178j |
| Phase Conductor 3 (Ph3) | 23.06076-1.52177j |
| Sky Wire 1 (Sk1) | 76.68306-1.51164j |
| Sky Wire 2 (Sk2) | 76.74379-1.51163j |
| Pipeline (MP) | 19.85862-1.56943j |

where $\overline{A}_z$ is the MVP on the surface of the pipeline and $l_m$ is the length of the pipeline.

In order to evaluate the self inductance of the pipeline, the same methodology is followed, except that now we impose a zero fault current $\overline{I}_F$ and a base current on the pipeline, for example $\overline{I}_{Pb} = 1000$ [A]:

$$L_{self} = \frac{\overline{A}_z \cdot l_m}{\overline{I}_{Pb}} \tag{3}$$

Applying a permutation of the fault current on each of the phases, by the exposed relations one can determine the mutual inductances between the faulted phase conductor and the MP. Assuming that the geometry of the system and the magnetic properties of both the pipeline and the phase conductor remain constant, the self and mutual inductances per unit length of all sections are equal.

Table III shows the results obtained for the self inductances per unit length of the studied system, with the metallic components separated by a distance of 30 [m] (between HVPL and MP), and an earth resistivity of 1000 [$\Omega$m].

For comparison, Table IV presents the results obtained for the self inductances per unit length of the studied system of metallic components for a 500 [m] distance between HVPL and MP, and an 100 [$\Omega$m] earth resistivity.

Having computed the impedances of the problem, a generalized equivalent circuit is constructed, as shown in Fig. 7.

Although it is not shown in this figure, the coupling between all conductors is taken into consideration. In the circuit representation, the ground wires are replaced with an equivalent metallic return path. In order to account for the fact that the pipeline coating is not perfect, (i.e. it has insulation defects), the pipeline is modeled in sections utilizing a series of grounding-leakage resistances. These resistances may also represent regular groundings used as a mitigation procedure, mainly ground or polarization cells. The equivalent electrical circuit can be solved based on standard methods from electrical circuit theory.

## V. Results

Solving the equivalent electrical circuit model attached to the studied geometrical configurations for the self and mutual im-

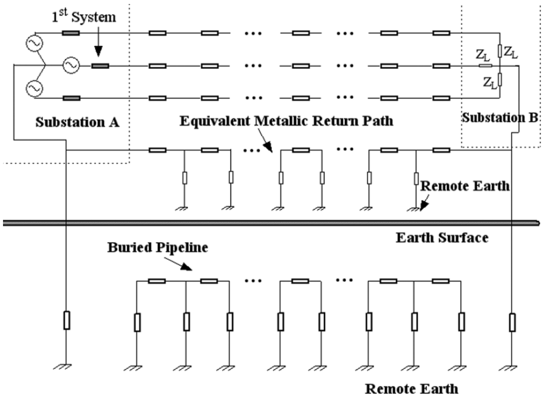


Fig. 7. Equivalent electrical circuit model for the investigated problem.

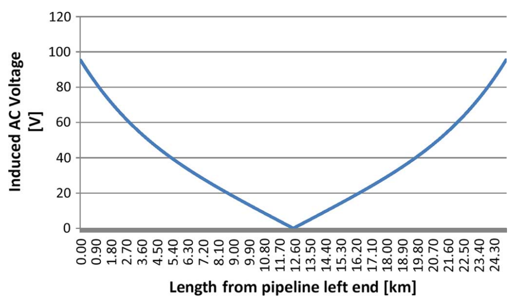


Fig. 8. Induced AC potential ($\mathrm{d} = 30$ [m] and $\rho = 100$ [$\Omega$m]).

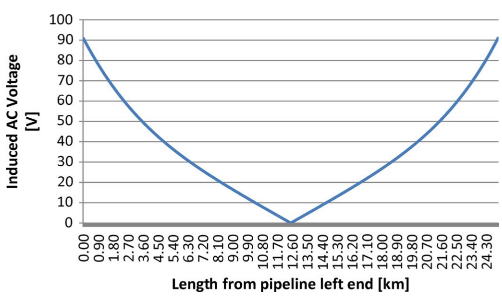


Fig. 9. Induced AC potential ($\mathrm{d} = 30$ [m] and $\rho = 1000$ [$\Omega$m]).

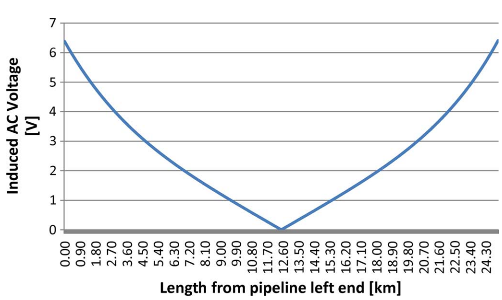


Fig. 10. Induced AC potential ($\mathrm{d} = 500$ [m] and $\rho = 100$ [$\Omega$m]).

pedances evaluated with MVP, which were determined on the surface of the system metallic components using the proposed neural network solution, the induced AC voltage can finally be calculated.

Fig. 8 presents the induced AC voltage in the underground metallic pipeline for a 30 [m] distance between HVPL and MP, and an 100 [$\Omega$m] earth resistivity.

One can observe that some high values for the induced voltage are obtained at both ends of the pipeline, which was expected due the fact that the pipeline is separated from the rest of the pipeline grid by two isolating junctions placed at its ends.

In Fig. 9 and 10 we present the induced AC voltages in the underground metallic pipeline for the two studied cases ($d = 30$ [m], $\rho = 1000$ [$\Omega$m]) and respectively ($d = 500$ [m], $\rho = 100$ [$\Omega$m]), in comparison with the results from Fig. 8.

From Figs. 9 and 10, one can observe that the separation distance between HVPL and ML has a greater influence on the induced AC voltage in the underground metallic pipeline than the earth resistivity.

## VI. Conclusions

From the results exposed in Figs. 3–6, one can see that absolute deviation of the solutions provided by the implemented NN, as to those provided by FEM, is almost insignificant for the training input data and somewhat higher, but still negligible for the testing input data.

The evaluation of the MPV for different geometrical configurations using neural networks proves to be a very effective technique, especially if we take into account the fact that the solutions provided by neural networks are obtained instantaneously, therefore reducing the computation time required by FEM.

Our contribution consists of implementing and effectively testing neural network AI technique (using MatLab software) to the study of the induced AC voltage in the underground metallic pipeline for different constructive geometries of the proposed problem.

In comparison with the neural network solution from [2] and [3], where the induced AC potential is directly evaluated, the authors of this paper propose a new neural network solution to evaluate MVP on the studied domain, using a larger training database for several different geometries.

The advantage consists in lower computational time, on a simplified calculus structure, with only a few input data. The intermediate results may also be used in other calculation. Afterwards, with a classical equivalent circuit, the final results may be obtained and verified.

## Acknowledgment

The authors are grateful to the Romanian Ministry of Scientific Research and Technology, for the financial support in the frame of the Research Projects ID_1024 and TE_253.

## References

[1] G. C. Christoforidis, D. P. Labridis, and P. S. Dokopoulos, "Inductive interference calculation on imperfect coated pipelines due to nearby faulted parallel transmission lines," *Elect. Power Syst. Res.*, vol. 6, no. 2, pp. 139–148, Aug. 2003.

[2] S. Al-Alawi, A. Al-Badi, and K. Ellity, "An artificial neural network model for predicting gas pipeline induced voltage caused by power lines under fault conditions," *COMPEL: Int. J. Comput. Math. Elect. Electron. Eng.*, vol. 24, no. 1, pp. 69–80, 2005.

[3] A. Al-Badi, K. Ellithy, and S. Al-Alawi, "Prediction of voltages on mitigated pipelines paralleling electric transmission lines using an artificial neural network," *J. Cor. Sci. Eng.*., vol. 10, Mar. 2007, 1466-8858, Preprint 28.

[4] D. P. Labridis, "Comparative presentation of criteria used for adaptive finite element mesh generation in multiconductor Eddy current problems," *IEEE Trans. Magn.*, vol. 36, no. 1, pp. 267–280, Jan. 2000.

[5] K. J. Satsios, D. P. Labridis, and P. S. Dokopoulos, "An artificial intelligence system for a complex electromagnetic fields problem: Part I and II—Finite element calculations and fuzzy logic development," *IEEE Trans. Magn.*, vol. 35, no. 1, pp. 516–527, Ja. 1999.